Enhanced Focusing Properties Using Surface Plasmon Multilayer Gratings

Hui Li
Lianshan Yan, Senior Member, IEEE
Zhen Guo
Wei Pan, Member, IEEE
Kunhua Wen
Hengyi Li
Xiangang Luo
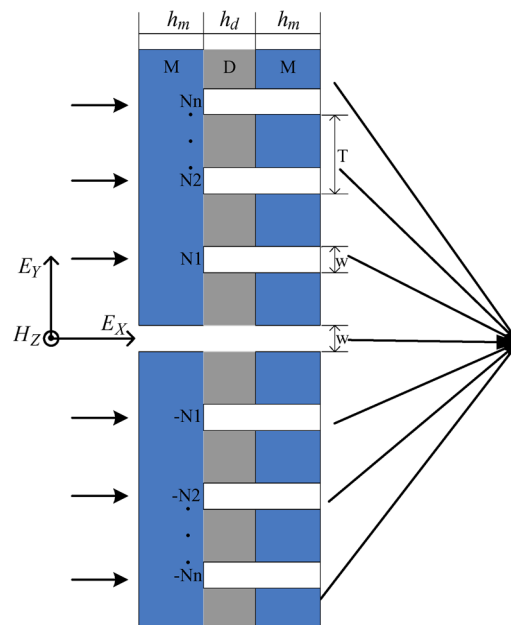
Enhanced Focusing Properties Using Surface Plasmon Multilayer Gratings

Hui Li,[1] **Lianshan Yan,**[1] *Senior Member, IEEE*, **Zhen Guo,**[1]
Wei Pan,[1] *Member, IEEE*, **Kunhua Wen,**[1] **Hengyi Li,**[2] **and Xiangang Luo**[2]

[1]Center for Information Photonics and Communications, School of Information Science and Technology, Southwest Jiaotong University, Chengdu 610031, China
[2]State Key Lab of Optical Technology for Microfabrication, Institute of Optics and Electronics, Chinese Academy of Science, Chengdu 610029, China

Abstract: A subwavelength slit with metal–dielectric–metal (MDM) composite surface gratings is proposed and numerically investigated using finite-difference time-domain (FDTD) method. Compared with conventional monometal-grating based structures, focusing properties of the proposed MDM structure can be enhanced based on multiple scattering and coupling of surface plasmon polaritons (SPPs) along the metal/dielectric multilayer films, especially the focal length can be varied from $\sim$2.6 to 5.82 μm by adjusting the dielectric thickness.

Index Terms: Gratings, multilayer interference coatings, plasmonics, subwavelength structures.

1. Introduction

Since Ebbesen first reported extraordinary optical transmission (Tr) through a 2-D metallic hole array in 1998 [1], there has been much interest in investigations about surface plasmon polaritons (SPPs) excited in subwavelength metallic structures, which opens up possibilities for designing new metallic nanophotonic devices [2]–[5]. Optical Tr of a 2-D array of subwavelength holes in a metal film was demonstrated with a significant increase in certain spectral ranges due to the excitation of surface polaritons [6]. A single subwavelength aperture or slit perforated on the metallic film surrounded by surface corrugations has attracted great attention due to not only its capability of handling light propagation but also its beaming effect in the far field [7], as well as the "lens like" properties [8], [9] for focusing light in the intermediate region (typically less than 2 μm). In addition to enhanced focusing approaches using slit-arrays [10], [11], recently, metal or/and dielectric multilayer structures have been theoretically investigated based on different mechanisms [12]–[15]. In [12], the focusing effect of a tapered subwavelength metal slit surrounded by surface dielectric gratings is manipulated by patterning surface corrugations on the output surface and regulating the aperture. In [15], the Tr efficiency is significantly enhanced using circular-type multilayer structures, while the focusing length is similar to conventional ones [7]. For certain applications, it would be highly desirable to increase focal lengths (FLs) and/or corresponding working distances, which is hardly doable using single-layer structures.

In this paper, we propose a metal–dielectric–metal (MDM) structure with a single slit flanked by grooves on the output side. Based on the effective excitation of SPP resonance modes in the MDM waveguide, focusing properties (i.e., the FL and the beam width at the focal point) of the transmitted light can be improved compared to conventional monometal grating structures [9] by tuning the dielectric thickness and/or other parameters. Simulation results based on the finite-difference time-domain (FDTD) method illustrate the enhancement of beam focusing. It is found that the far-field enhancement at the focal point originates not only from SPP-assisted diffraction process along the propagation direction of the incident light but from multiple scattering and coupling of SPPs along the metal/dielectric multilayer films as well. Such design may find applications in micro- or nano-fabrications, lithography, smart antennas, etc.

2. Theoretical Analysis and Structure

The basic principle of the proposed structure is based on the interference modulation of SPPs. For periodically modulated metal films, this can be expressed using the wave-vector of the grating. On the exiting side of the structure, diffraction of the incident light will happen. The diffraction angle θ, which is determined by the propagation constant of EM mode in the multilayer slits and the reciprocal vector of the metal grating, can be calculated by the grating equation in [16]

$$k_{sp} \pm m\frac{2\pi}{T} = k_0\sin\theta \qquad (1)$$

where k_{sp} represents the wave vector of SP, k_0 is the wave vector in free space, and T is the period of the grating. To realize beam focusing of the input light, we assume that the diffraction angle $\theta = 0$. Equation (1) can be regarded as the coupling condition between the surface waves vector k_{sp} and the free space wave vector k_0.

Unlike monometal structures, the grating structure proposed in this paper is a metal–dielectric composite grating deposited on the metal film. It is well known that a light wave tends to localize itself mostly in a medium with higher refractive index and propagate with low phase velocity [17]. Subsequently, as the incident light transmits through the dielectric layer sandwiched between metal layers, SPPs will be generated along the interfaces. For such an MDM waveguide, as the two closely placed parallel metallic plates are filled with the dielectric layer with higher refractive index, the complex propagation constant $(k_{sp} = k'_{sp} + ik''_{sp})$ can be calculated as [16]–[20]

$$\tanh(k_d h_d/2) = -\frac{\varepsilon_d k_m}{\varepsilon_m k_d}. \qquad (2)$$

Here, $k_m = \sqrt{k_{sp}^2 - \varepsilon_m k_0^2}$ and $k_d = \sqrt{k_{sp}^2 - \varepsilon_d k_0^2}$ represent the wave vector in the metal and dielectric layer, respectively. h_d is dielectric thickness. ε_m and ε_d are the relative permittivity of the metal and the dielectric (the metal is treated as a dielectric with a complex-value permittivity), respectively. The propagation constant and the effective index of the MDM waveguide are important to validate the simulation results. Similar to the case of conventional dielectric waveguides, the number of SPP modes supported by the waveguide increases with thicker dielectric layer. Using (2), one may note that for $h_d \ll \lambda$, an MDM waveguide supports only a single antisymmetric mode [21]. When the dielectric thickness h_d increases to the scale of the resonant length, more energy could be stored in the cavity (the central dielectric layer) to enhance the Tr. Hence, the focusing performance may be improved by manipulating parameters of output gratings.

Fig. 1 illustrates the proposed structure, where a nanoslit with width w is introduced in the center of the metal film with thickness h_m. The number of grooves at either side of the slit is n. The right surface is covered by metal–dielectric composite surface gratings with dielectric thickness h_d and metal-coating thickness h_m, and the period of the grating is T. When a transverse magnetic (TM)-polarized plane wave with its wavelength $\lambda = 193$ nm illuminates normally from the left side of the slit, it couples into SPPs, diffracts at the output surface, and further propagates in the air. Part of the diffracted EM wave on the output surface, may propagate along the waveguide as well. Since the input and output gratings are responsible for the Tr enhancement and the beam focusing effect
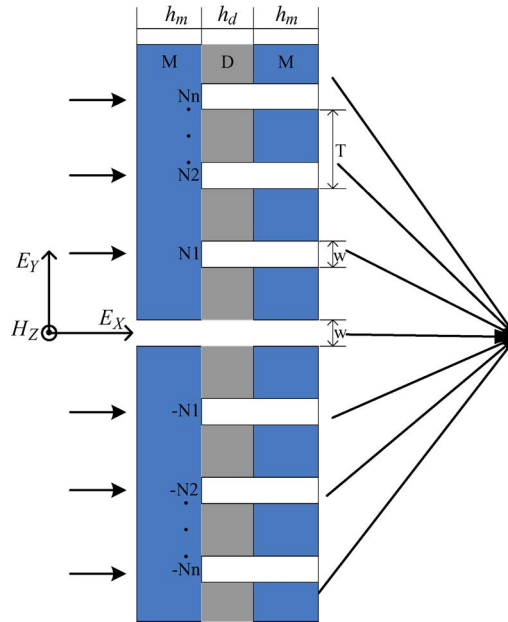
Fig. 1. Schematic diagram of the proposed structure: The output surface is covered by a metal–dielectric composite grating with a period T. The thickness values of the dielectric and metal coating are h_d and h_m, respectively. The input light is a TM-polarized plane wave from the left.

independently, we concentrate on the design or optimization of geometrical parameters of the output surface. The key performance characteristics of focusing, such as Tr, FL, full-width at half-maximum (FWHM) of the E-field intensity along the y-direction at the focal point, and the depth of focusing (DOF), are investigated. Although most of these parameters are well-defined in the literature, to be more specific, DOF is defined as the distance between the points with $(1 - 1/e^2)$ intensity of the focal point at both sides in our simulations. Note that the DOF parameter also indicates the working distance for beaming applications.

3. Simulation Results and Discussion

In order to investigate focusing properties of the proposed structure, we use finite-difference time-domain (FDTD) method. Metal films at both sides of the structure are set to have identical lengths with the thickness $h_m = 20$ nm. The period of the grating is set to $T = 100$ nm (an optimal value based on numerous simulations). The whole length of the structure in the y-direction (see Fig. 1) is 1.5 μm. In addition, the permittivity values of the dielectric and metal material are $\varepsilon_{MgO} = 4.08$ and $\varepsilon_{Al} = -4.43 + 0.4985i$, respectively, [22]. The simulation region is surrounded by Perfectly Matched Layers (PML) to prevent any unwanted back reflections. The spatial step size in the simulations is set to 0.5 nm. In addition, two power monitors are placed at the input and output side of the grating for calculating the incident power (i.e., P_{in}) and the transmitted power (i.e., P_{out}). Subsequently, the Tr is defined to be Tr = P_{out}/P_{in}.

3.1. F-P Cavity Effect of the Multilayer Grating

The thickness of the dielectric layer h_d is one of the key performance parameters. Fig. 2 shows the far-field Tr pattern versus the dielectric thickness h_d for two different numbers of grooves (i.e., $n = 1$ and 5). Four sharp peaks can be observed, which illustrate the F-P cavity effect as SPPs travel in the middle dielectric layer with a finite thickness. The cavity effect can be viewed as multiple light reflections occurred at two interfaces due to the impedance mismatch between the dielectric and metal materials. To show such effect in details, we simply calculate the transmittance by varying the thickness of the dielectric layer. As clearly shown in Fig. 2(a), the transmittance
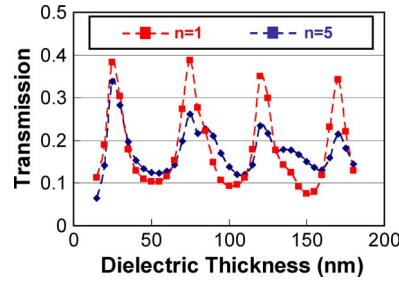
Fig. 2. Far-field transmission pattern of the proposed structure with different number of grooves ($n = 1, 5$). Other parameters: $w = 20$ nm, and $T = 100$ nm.
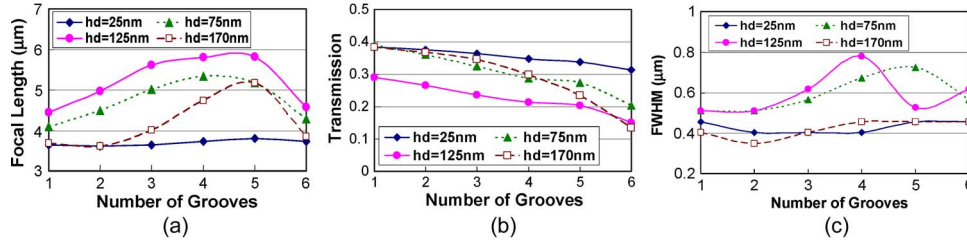

Fig. 3. Simulation results. (a) Focal length. (b) Transmission. (c) FWHM at the focal point as a function of the groove number with different dielectric thickness (25, 75, 125, and 170 nm).
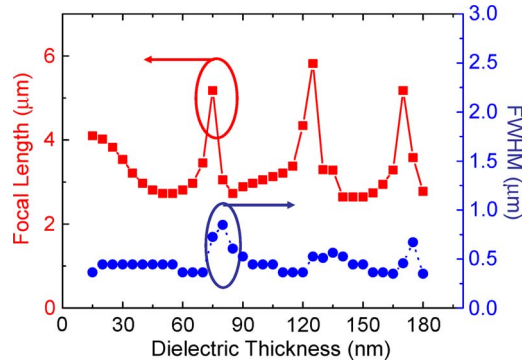

Fig. 4. Focal length and FWHM at the focal point with varied dielectric thickness (the groove number $n = 5$).

exhibits a periodic pattern as a function of the dielectric thickness, and the period of ~50 nm coincides with half of the SPP wavelength determined by $\lambda_{spp} = 2\pi / k_{spp}$ [i.e., referring to (1)]. On the other hand, the overall Tr monotonically decreases with increased dielectric thickness, mainly due to more insertion loss.

3.2. Groove Number and Dielectric Thickness

As the number of grooves increases, the FL, Tr, and FWHM will change as well, as illustrated in Fig. 3(a)–(c) with different dielectric thickness values (utilizing the maximum Tr pattern in Fig. 2, i.e., $h_d = 25, 75, 125,$ and 170 nm). When the dielectric thickness is small (e.g., 25 nm), the focusing performance changes slightly with different groove numbers, while it varies evidently as the thickness becomes larger (e.g., 75, 125, and 175 nm). Here, the cavity resonance may play a key role in the enhancement of electromagnetic field when the dielectric thickness is small and, subsequently, the influence of groove number is negligible.
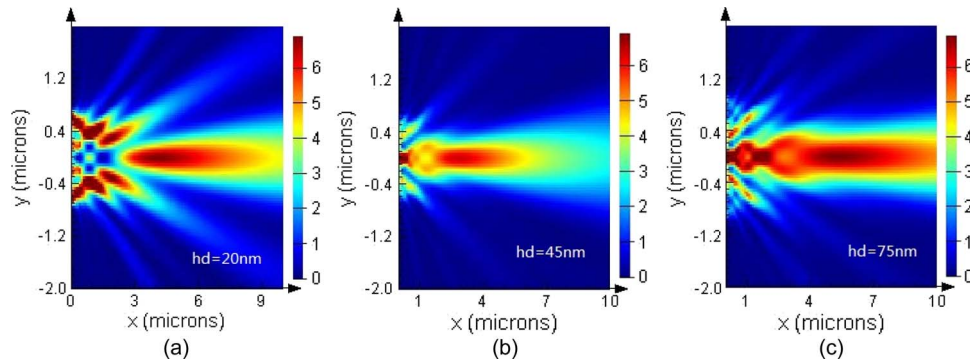
Fig. 5. Profiles of E-field intensity of the proposed structure with different dielectric thickness (a) $h_d = 20$ nm, (b) $h_d = 45$ nm, and (c) $h_d = 75$ nm.
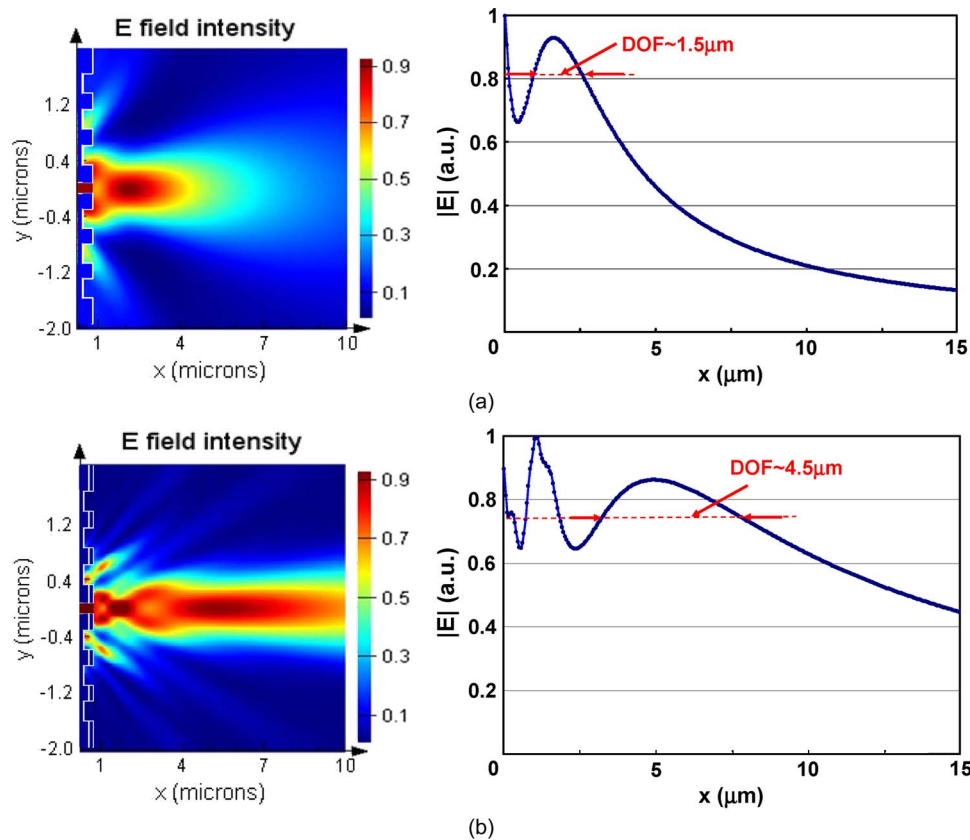

Fig. 6. E-field distribution (left) and the depth of focusing (DOF, right) of (a) monometal structure and (b) metal–dielectric–metal structure with the dielectric thickness of 125 nm.

We then set the groove number as 5 (i.e., $n = 5$) and vary the dielectric thickness only (note that the whole thickness of the structure will change accordingly). Fig. 4 illustrates the calculated values of the FL and the beam width (i.e., FWHM). Obviously, the tendency of the FL agrees with that of the Tr. The minimum value of the FWHM is ~ 0.35 μm, while the FL ranges from ~ 2.6 μm to 5.82 μm.

Fig. 5(a)–(c) further illustrate the corresponding E-field intensity distributions for three different values of h_d. The E-field intensity distribution results show that the energy emerging from the structure tends to focus within several micrometers in an extremely small region (i.e., small FWHM).
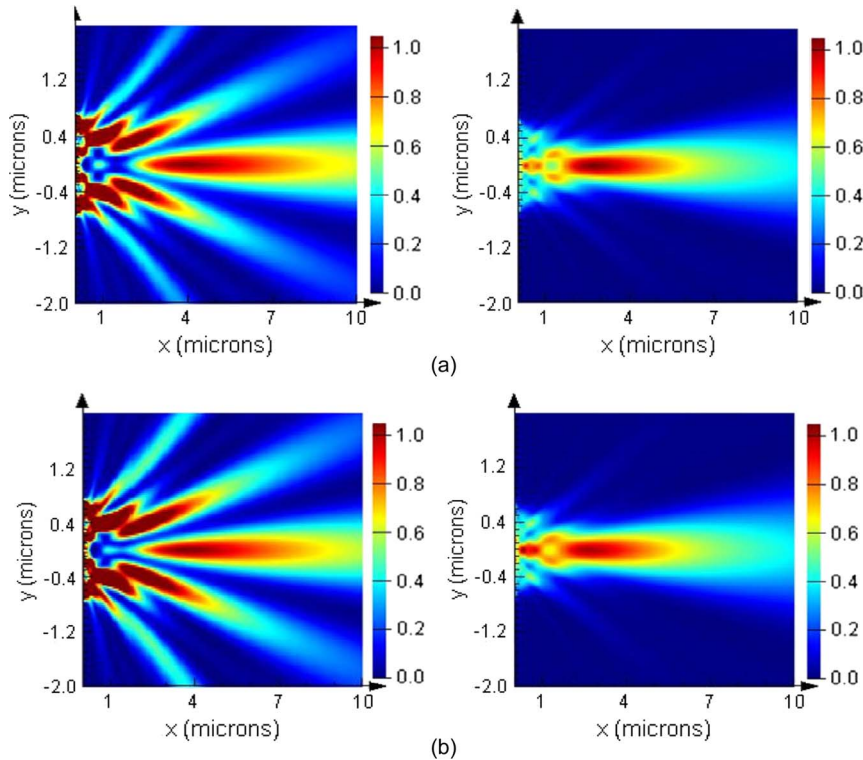
Fig. 7. Focusing properties of proposed MDM grating structure with different dielectric materials ($n = 5$). (a) SiO_2 and (b) GaF, with $h_d = 25$ nm (left) and $h_d = 75$ nm (right).

For example, the case with $h_d = 20$ nm shown in Fig. 5(a) reveals an FL of 3.8 μm and the corresponding FWHM of 0.44 μm. When h_d increases to 45 nm, the FL reduces to 2.8 μm [see Fig. 5(b)]. For the case with $h_d = 75$ nm, the FL increases to 5.2 μm with a larger FWHM value of ~0.7 μm [see Fig. 5(c)]. Fig. 5(a)–(c) are also in accordance with the Tr trace in Fig. 2.

3.3. MDM Versus Monometal Structure

To compare focusing properties of the optimized structure with previous monometal structures, we further illustrate two E-field intensity distributions in Fig. 6, with Fig. 6(a) for monometal structure that agrees well with results in [9] (parameters used in [9]: The thickness of the silver film is $h_d = 200$ nm, the width of the slit and all grooves is $w = 200$ nm, the groove period is $T = 420$ nm, and the groove number is $n = 3$ at each side) and Fig. 6(b) for the proposed structure with $h_d = 125$ nm. The FLs in Fig. 6(a) and (b) are ~2 μm and ~5.82 μm, respectively. Moreover, the DOF of the proposed structure is about three times longer than that of the monometal structure (i.e., 4.5 versus 1.5 μm). This clearly verifies better focusing properties using the MDM multilayer structure over conventional monometal structures. Such improvement is mostly due to enhanced excitation at metal/dielectric and dielectric/metal interfaces, as well as more effective coupling in the dielectric layer. These characteristics are very important for various applications such as nanofabrications or optical lithography, etc., as the new structure can provide longer working distance.

3.4. Dielectric Materials

Furthermore, we highlight the importance of proper dielectric material selection. As indicated by (2), the complex propagation constant (K_{spp}) and effective refractive index (n_{eff}) of SPPs increases until the dielectric permittivity (ε_d) approaches $|Re(\varepsilon_m)|$. Particularly, the frequency at which $\varepsilon_d = |Re(\varepsilon_m)|$ is called the resonant surface plasmon frequency. For the chosen metal, we have

$|\text{Re}(\varepsilon_m)| = 4.43$, which is close to ε_{MgO} (i.e., 4.08). Therefore, the MgO layer we used is predicted to meet the closest resonance condition. As a comparison, we simulate another two popular dielectric materials, i.e., SiO2 and GaF, with $\varepsilon_{sio2} = 2.35$ and $\varepsilon_{GaF} = 2.255$ [22], [23]. Fig. 7(a) and (b) compare the E-field distributions of two dielectric materials (here, n = 5) with $h_d = 25$ nm (left) and 75 nm (right), respectively. Apparently, the emitting light diverges quickly with poor focusing effect when the dielectric thickness is low (i.e., 25 nm), while the far-field E-intensity starts to concentrate on the main lobe but still with much shorter FL and the DOF for larger thickness (i.e., 75 nm). Therefore, we can easily choose the optimized materials for layers (both dielectric and metal) based on above guideline.

4. Conclusion

In conclusion, a multilayer grating structure to improve the performance of focusing in a single subwavelength slit was proposed. Not only the SPPs-assisted diffraction, but the coupling and scattering between layers as well, contribute to the focusing enhancement. Numerical simulation results indicate that the beam focusing effects are governed by several structural parameters: the thickness of the dielectric layer and the period of grooves. A flexible FL (from 2.6 μm to 5.82 μm) with comparable beam width is feasible using appropriate parameters. Such a design may be helpful for designing subwavelength optical devices, as well as facilitating manufacturing processes.

References

[1] T. W. Ebbesen, H. J. Lezec, H. F. Ghaemi, T. Thio, and P. A. Wolff, "Extraordinary optical transmission through sub-wavelength hole arrays," *Nature*, vol. 391, pp. 667–669, Feb. 1998.

[2] A. Yanai and U. Levy, "Plasmonic focusing with a coaxial structure illuminated by radially polarized light," *Opt. Exp.*, vol. 17, no. 2, pp. 924–932, Jan. 2009.

[3] W. L. Barnes, A. Dereux, and T. W. Ebbesen, "Surface plasmon subwavelength optics," *Nature*, vol. 424, no. 2, pp. 824–830, Aug. 2003.

[4] J. J. Mock, S. J. Oldenburg, D. R. Smith, D. A. Schultz, and S. Schultz, "Composite plasmon resonant nanowires," *Nano Lett.*, vol. 2, no. 5, pp. 465–469, 2002.

[5] Y. Yu and H. Zappe, "Effect of lens size on the focusing performance of plasmonic lenses and suggestions for the design," *Opt. Exp.*, vol. 19, no. 10, pp. 9434–9444, May 2011.

[6] L. Salomon, F. Grillot, A. V. Zayats, and F. de Fornel, "Near-field distribution of optical transmission of periodic subwavelength holes in a metal film," *Phys. Rev. Lett.*, vol. 86, no. 6, pp. 1110–1113, Feb. 2001.

[7] W. Song, Z. Fang, S. Huang, F. Lin, and X. Zhu, "Near-field nano-focusing through a combination of plasmonic Bragg reflector and converging lens," *Opt. Express*, vol. 18, no. 14, pp. 14 762–14 767, Jul. 2010.

[8] F. J. Garcia-Vidal, L. Martin-Moreno, H. J. Lezec, and T. W. Ebbesen, "Focusing light with a single subwavelength aperture flanked by surface corrugations," *Appl. Phys. Lett.*, vol. 83, no. 22, pp. 4500–4502, Oct. 2003.

[9] H. Shi, C. Du, and X. Luo, "Focal length modulation based on a metallic slit surrounded with grooves in curved depths," *Appl. Phys. Lett.*, vol. 91, no. 9, p. 093111, Aug. 2007.

[10] L. Verslegers, P. B. Catrysse, Z. Yu, J. S. White, E. S. Barnard, M. L. Brongersma, and S. Fan, "Planar lenses based on nanoscale slit arrays in a metallic film," *Nano Lett.*, vol. 9, no. 1, pp. 235–238, Jan. 2009.

[11] T. Sondergaard, S. I. Bozhevolnyi, S. M. Novikov, J. Beermann, E. Devaux, and T. W. Ebbsesen, "Extraordinary optical transmission enhanced by nanofocusing," *Nano Lett.*, vol. 10, no. 8, pp. 3123–3128, Aug. 2010.

[12] G. Zheng, L. Shi, H. Wang, and X. Li, "Beam focusing through a tapered subwavelength aperture surrounded by dielectric surface gratings," *Opt. Comm.*, vol. 282, no. 20, pp. 4146–4151, Oct. 2009.

[13] Y. Liu, H. Shi, C. Wang, C. Du, and X. L. Luo, "Multiple directional beaming effect of metallic subwavelength slit surrounded by periodically corrugated grooves," *Opt. Exp.*, vol. 16, no. 7, pp. 4487–4493, Mar. 2008.

[14] A. Y. Nikitin, F. J. García-Vidal, and L. Martín-Moreno, "Enhanced optical transmission, beaming and focusing through a subwavelength slit under excitation of dielectric waveguide modes," *J. Opt. A, Pure Appl. Opt.*, vol. 11, no. 12, p. 125 702, Dec. 2009.

[15] H. C. Kim, H. Ko, and M. Cheng, "High efficient optical focusing of a zone plate composed of metal/dielectric multilayer," *Opt. Exp.*, vol. 17, no. 5, pp. 3078–3083, Feb. 2009.

[16] L. B. Yu, D. Z. Lin, Y. C. Chen, Y. C. Chang, K. T. Huang, J. W. Liaw, J. T. Yeh, J. M. Liu, C. S. Yeh, and C. K. Lee, "Physical origin of directional beaming emitted from a subwavelength slit," *Phys. Rev. B, Condens. Matter*, vol. 71, no. 4, p. 041405, Jan. 2005.

[17] P. K. Tien, "Integrated optics and new wave phenomena in optical waveguides," *Rev. Mod. Phys.*, vol. 49, no. 2, pp. 361–420, Apr.–Jun. 1977.

[18] R. Zakharian, J. V. Moloney, and M. Mansuripur, "Surface plasmon polaritons on metallic surfaces," *Opt. Exp.*, vol. 15, no. 1, pp. 183–197, Jan. 2007.

[19] B. Wang and G. P. Wang, "Plasmon Bragg reflectors and nanocavities on flat metallic surfaces," *Appl. Phys. Lett.*, vol. 87, no. 1, p. 013107, Jun. 2005.

[20] P. Lalanne and J. Hugonin, "Interaction between optical nano-objects at metallic–dielectric interfaces," *Nature Phys.*, vol. 2, pp. 551–556, Jul. 2006.

[21] A. Pannipitiya, I. D. Rukhlenko, M. Premaratne, H. T. Hattori, and G. P. Agrawal, "Improved transmission model for metal–dielectric–metal plasmonic waveguides with stub structure," *Opt. Exp.*, vol. 18, no. 6, pp. 6191–6204, Jun. 2010.

[22] D. M. Roessler and D. R. Huffman, "Magnesium oxide (MgO)," in *Handbook of Optical Constants of Solid II*, E. D. Palik, Ed. Orlando, FL: Academic, 1991, pp. 919–956.

[23] D. M. Roessler and D. R. Huffman, "Silicon dioxide (SiO2)," in *Handbook of Optical Constants of Solids*, E. D. Palik, Ed. New York: Academic, 1985, pp. 749–752.